

Analysis of Fluid Structural Instability in Water

CONF-970233--

N. Piccirillo

February 1997

DISTRIBUTION OF THIS DOCUMENT IS UNLIMITED



MASTER

NOTICE

This report was prepared as an account of work sponsored by the United States Government. Neither the United States, nor the United States Department of Energy, nor any of their employees, nor any of their contractors, subcontractors, or their employees, makes any warranty, express or implied, or assumes any legal liability or responsibility for the accuracy, completeness or usefulness of any information, apparatus, product or process disclosed, or represents that its use would not infringe privately owned rights.

KAPL ATOMIC POWER LABORATORY

SCHENECTADY, NEW YORK 12311

Operated for the U. S. Department of Energy
by KAPL, Inc. a Lockheed Martin company

DISCLAIMER

This report was prepared as an account of work sponsored by an agency of the United States Government. Neither the United States Government nor any agency thereof, nor any of their employees, make any warranty, express or implied, or assumes any legal liability or responsibility for the accuracy, completeness, or usefulness of any information, apparatus, product, or process disclosed, or represents that its use would not infringe privately owned rights. Reference herein to any specific commercial product, process, or service by trade name, trademark, manufacturer, or otherwise does not necessarily constitute or imply its endorsement, recommendation, or favoring by the United States Government or any agency thereof. The views and opinions of authors expressed herein do not necessarily state or reflect those of the United States Government or any agency thereof.

DISCLAIMER

Portions of this document may be illegible in electronic image products. Images are produced from the best available original document.

ANALYSIS OF FLUID-STRUCTURAL INSTABILITY IN WATER

N. Piccirillo
Lockheed Martin Corporation
P.O. Box 1072
Schenectady, NY 12301-1072

ABSTRACT

Recent flow testing of stainless steel hardware in a high pressure / high temperature water environment produced an apparent fluid-structural instability. The source of instability was investigated by studying textbook theory and by performing NASTRAN finite element analyses. The modal analyses identified the mode that was being excited, but the flutter instability analysis showed that the design is stable if minimal structural damping is present. Therefore, it was suspected that the test hardware was the root cause of the instability. Further testing confirmed this suspicion.

NOMENCLATURE

a = Measured acceleration in micro g's
 B = Structural Damping (matrix)
 C_m = Coefficient of Moment at an angle β . For small changes in β , C_m is expressed using the first two terms of the Taylor Series expansion $C_M + \Delta\beta \cdot dC_M/d\beta$ where $dC_M/d\beta$ is evaluated at the initial value for β . If $\beta \sim 0$ initially, then $C_M = 0$.
 dB = Acceleration expressed in decibels relative to a micro g
 D = Thickness of plate extension = 0.67"
 $F(t)$ = Forcing function
 F_θ = Fluid Force at some angle θ
 $f_{(f+s)}$ = Natural frequency in a fluid in cycles/sec (Hz)
 H = Height of plate extension = 20.60"
 J = Polar mass moment of inertial about the pivot including fluid mass moment of inertia
 K_θ = Torsional structural stiffness constant per unit length of the section
 K = Structural stiffness (matrix)
 L = length of plate extension parallel to flow = 7.03"
 M = Mass (matrix)
 M_f = Hydromass contribution to the mass matrix
 n = exponent relating measured acceleration vs. flow velocity
 M_s = Structural mass contribution to mass matrix
 R = Characteristic radius about the pivot point
 V = Fluid cross flow velocity
 V_c = Critical flow velocity for instability

V_{rel} = Relative Fluid Velocity due to rotation of a plate
 t = time

θ = Rotation of plate

$\beta, \Delta\beta$ = Relative flow angle of attack to plate, change in relative flow angle due to plate oscillations

ζ_o = Damping ratio for a given natural frequency

ρ_f = Density of the fluid = 49 lb_m/ft³ from Reference (1) for water at a reference temperature of 500°F

ρ_s = Density of structure = 488 lb_m/ft³ for Type 304 stainless steel from Reference (1)

$\omega(s)$ = Eigenvalues of the structure in rad/sec

$\omega(f+s)$ = Eigenvalues of the structure in a fluid in rad/sec

1.0 INTRODUCTION

A fluid-structural instability can result in fatigue concerns, wear, and eventually structural failure. Therefore, such instabilities of a structure must be avoided. Recently, a stainless steel structure was flow tested in a high pressure / high temperature water flow environment and displayed instability characteristics.

A fluid-structural instability which is related to the structural design would require a redesign which may impact cost and scheduling. Testing alone does not always indicate sources and potential fixes for problems such as fluid-structural instabilities. Meaningful analytical studies can often lead to further understanding of the problem which will minimize its ultimate impact. Analytical studies for this fluid-structural instability investigation included the following:

1. Assessment and application of textbook theory.
2. NASTRAN Finite Element Methods (FEM): Normal modes analyses (wet and dry).
3. NASTRAN FEM: Aerodynamic flutter analyses (Reference (6)).

Textbook theory was used to provide basic understanding and baseline predictions for comparison to finite element analyses. The NASTRAN normal modes results can be used to compare with modal test results, to indicate the probable

mode that goes unstable, and to better understand the effect of a water environment on normal modes. NASTRAN Aerodynamic Flutter analysis results are compared to test results in order to assess whether the fluid-structural instability is design related and to identify potential design improvements.

2.0 EXPERIMENTATION

2.1 Test Equipment and Parameters

The flow test was performed in a small pressurized vessel at high temperature. The structure being tested included a cantilevered plate extension extending from a much stiffer main component of interest (Figure 1). The test was conducted in water with variable cross flow rate, and variations in angles of attack controlled by rotating the test fixture in the test vessel. A set of acoustic pressure transducers and accelerometers were used to record parameters on the main component.

2.2 Detection of a Fluid-Structural Instability

The following three characteristics in a flow test could indicate a fluid structural instability:

1. Noise propagating to most accelerometers
2. Sharp amplitude at a resonance frequency (i.e. low damping)
3. The exponential relationship between measured acceleration and flow velocities increasing rapidly beyond the typical range for turbulent flow.

Figures (2) is an idealized spectra of acceleration showing a probable instability. It depicts a growing signal at 800 Hz as a function of flow rate developing into a sharp peak. The growing signal is also depicted in a plot of acceleration versus flow velocity as shown in Figure 3 (similar to Reference (5) Fig. 5.2). If the signal strength (a) varies with the flow velocity (v) raised to a constant power (n), then a normal-log plot of dB versus flow velocity appears as a straight line with the slope signifying the exponent (n). Consider a signal strength:

$$a(v) \sim V^n \quad (1)$$

When $a(v)$ is specified in dB:

$$dB - (n \cdot 20 \log(V)) \quad (2)$$

A typical stable value for (n) is two (i.e. dipole) based on drag and lift forces on a plate which are proportional to acceleration. However, (n) may be as high as four (i.e. quadruple) for vibrations induced by turbulence (Reference (5)). In Figure (3), $n=9$ signifies a potential fluid-structural instability.

2.3 Experimental Test Results

2.3.1 Flow Testing

During the flow test, an unexpected fluid-structural instability of the test piece was excited. A tone at 800 Hz (varying somewhat with flow angle) was observed at flow rates of 90-180 inches / second and cross flow angles of $+45^\circ$ to -45° . The tone satisfied the three characteristics for instability noted in section 2.2 and was believed to be a resonance of the plate extension.

2.3.2 Modal Impact and Shaker Tests

Modal impact and shaker tests were performed to determine which structural mode became unstable and damping ratios. The modal impact test results predicted a complex bending and torsional mode of the plate extension at 887 Hz. The shaker test predicted the same mode at 871 Hz (dry) and 800 Hz (wet). Based on these results, analyses focused on this mode as the probable instability source. Shaker test critical damping ratios were 0.17-0.52% (dry) and 1.0-2.8% (wet).

3.0 ANALYSIS

3.1 Wet Modal Analysis Theory

Resonant frequencies are expected to shift in a water environment. Water affects the viscous damping of the structure and adds hydromass to it. Below are some fundamental equations to predict how hydromass shifts the structural modes in water. Because the fluid-structural instability occurred in water, it is important to correlate dry modal frequencies to corresponding wet modal frequencies.

The characteristic equation of motion for an oscillating system is:

$$M \frac{d^2 x}{dt^2} + B \frac{dx}{dt} + Kx = F(t) \quad (3)$$

where x is the displacement in a given direction. For a dry undamped normal modes analysis:

$$M = M_s - \rho_s L D H \quad (4)$$

$$B = F(t) = 0 \quad (5)$$

Equation (3) is reduced to:

$$\frac{d^2 x}{dt^2} + \omega^2 x = 0 \quad (6)$$

$$\omega = \omega(s) = M_s^{-1} K \quad (7)$$

For a structure in a fluid such as water, additional mass is applied to the mass matrix M depending on the direction of motion. For the x (non-stiff orientation) and y (stiff orientation) directions in Figure 1, the hydromass contribution to the mass matrix, M_f , is calculated from Reference (2) as:

$$M_f(x) = \frac{1.14 \rho_f \pi L^2 H}{4} \quad (8)$$

$$M_f(y) = \frac{2.23 \rho_f \pi D^2 H}{4} \quad (9)$$

The coefficients 1.14 and 2.23 are derived as functions of the geometry with respect to the direction of motion of a particular

mode. The eigenvalues in a fluid, $\omega(f+s)$, become:

$$\omega_x(f+s) \sim \left(\sqrt{\frac{M_s}{M_f(x) + M_s}} \omega_x(s) \right) \quad (10)$$

$$\omega_y(f+s) \sim \left(\sqrt{\frac{M_s}{M_f(y) + M_s}} \omega_y(s) \right) \quad (11)$$

3.2 Instability Analysis Theory: Flutter or Galloping

The fluid-structural instability encountered during the flow test may have been due to a phenomenon known as flutter or galloping instability. "Flutter" is best known as a phenomenon in aircraft wing design. Recently, a flutter analysis of an aircraft fin was presented in Reference (3). A flow-induced vibration instability of a blade suspended in a water flow channel was investigated in Reference (4).

The theory for flutter or galloping instability, as described in Reference (5), was studied to assess if and how this phenomenon could take place in the flow test conditions. The onset of instability occurs when zero damping is reached for a particular mode. The damping of the structure changes with flow velocity and angle of attack due to the fluid force that a structure with non circular cross section experiences. As a structure vibrates, its orientation changes slightly and the fluid forces oscillate. These oscillating forces generally tend to return the structure to its starting location. However, if there is a negative system damping, the oscillating fluid forces increase displacements and the structure is unstable. If the structure is unstable, very large amplitudes can result.

An instability may be either translating, rotational, or both. Figure 4 shows a 2D free body diagram for rotational stability of a plate exposed to a steady flow. Reference (5) determines the following relationships for a small $\Delta\beta$:

$$\beta = (-\theta + \Delta\beta) = \left(-\theta + \frac{Fd\theta}{Vdt} \right) \quad (12)$$

$$V \sim V_{rel} \quad (13)$$

The equation of motion (3) is rewritten for torsion and the fluid force as follows:

$$\begin{aligned} J \frac{d^2\theta}{dt^2} + B \frac{d\theta}{dt} + K_\theta \theta &= F(t) = \frac{\rho V^2 D^2 C_m}{2} \\ &= \frac{\rho V^2 D^2}{2} \left(\frac{\partial C_M}{\partial \beta} (\beta=0) \right) \beta \end{aligned} \quad (14)$$

By relating the terms in equations (12) and (14), the motion equation can be rewritten as:

$$J \frac{d^2\theta}{dt^2} + \left(B - \frac{\rho V R D^2}{2} \left(\frac{\partial C_M}{\partial \beta} \right) \right) \frac{d\theta}{dt} + \left(K_\theta + \frac{\rho V^2 D^2}{2} \left(\frac{\partial C_M}{\partial \beta} \right) \right) \theta = 0 \quad (15)$$

The $d\theta/dt$ terms represent the total system damping. The

structural damping, B, may also be written as:

$$B = 2J\zeta_o \omega_{(f+s)} = 4\pi J f_{(f+s)} \zeta_o \quad (16)$$

Equation (15) reveals that if C_M increases with increasing angle of attack, the total system damping term may decrease and eventually reach zero. The critical flow velocity at which the system damping reaches zero is calculated by setting the $d\theta/dt$ terms to zero and substituting Equation (16) into (15):

$$\frac{V_c}{f_{(f+s)} D} = \left(\frac{4 J (2\pi\zeta_o)}{\rho_f D^3 R} \right) \left(\frac{dC_M}{d\beta} \right) \quad (17)$$

By calculating J in terms of ρ_s , L, and D and substituting $R=L/2$, equation (17) can be reduced to:

$$\frac{V_c}{f_{(f+s)} D} = \left(\left(\frac{4\pi\rho_s \zeta_o}{3\rho_f} \right) \left(1 + \frac{L^2}{D^2} \right) \right) \left(\frac{dC_M}{d\beta} \right) \quad (18)$$

Equation (18) can be solved for several ways. For instance, if the structural damping is known, then V_c may be solved for. Similarly, if there is a particular velocity of interest, then the amount of damping caused by that fluid flow may be calculated. That value would also indicate the positive structural and/or viscous damping required to prevent an instability.

3.3 Finite Element Modeling

A 3-D NASTRAN FEM model of the plate extension was constructed to calculate dry and wet normal modes. The plate extension model was constrained at the bottom where the main component would be (not modeled). The wet modal analysis required 2-D MFLUID (i.e. virtual mass) elements which were constructed coincident to the exterior surface of 3-D solid elements in contact with water. NASTRAN calculated the hydromass based on user specified fluid density for the wetted side of the MFLUID elements.

The 3-D NASTRAN model was also used to perform a flutter analysis. This model was extended to include an aerodynamic surface parallel to the flow direction which is defined by grid points. The fluid forces were defined for the aerodynamic surface and superimposed onto the structural model by the FEM code. For each flow velocity selected, NASTRAN solved for complex eigenvalues and the damping associated with each mode of interest.

The P-K option was used for the NASTRAN aeroelastic analysis which is described in Reference (6). This option uses a double lattice method based on linearized potential flow theory of evaluating the fluid forces. This theory is applicable for thin bodies where there is little drag and for a small fluid flow angle, $\beta=0$. Other modeling assumptions included:

- The flow encounters no obstructions such as instrumentation or adjacent structures
- There are no viscous/flow separation/cavitation effects
- Pure cross flow takes place
- The main component is rigid
- Contributions of fluid acoustical resonances were insignificant

4.0 RESULTS

4.1 Normal Modes Analysis

Equations (10) and (11) were solved for the plate extension geometry as follows:

$$\omega_x(f+s) = 0.72\omega_x(s)$$

$$\omega_y(f+s) = 0.99\omega_y(s)$$

The conclusion is that mode shapes whose deflections are in the non-stiff directions may be reduced by as much as 28% while those in the stiff direction may not be reduced at all.

The NASTRAN modal analysis was done for a frequency range of 0-1100 Hz. Table 1 details the modes and mode shapes determined for both a dry and wet modal analysis. The percent reductions agree well with expectations based on textbook theory. A complex bending and torsional mode predicted at 833 Hz (Mode 5) is believed to be the mode associated with the experimental instability. The mode shape at 833 Hz is shown in Figure 5. These analytical predictions also agreed well with model test and shaker test results.

4.2 Flutter Analysis

Equation (18) was solved for the plate extension. For flow parallel to the long side of the plate ($\beta=0$), Reference (5) specifies $dC_M/d\beta = 26$. At a flow velocity of 150 inches/sec and a structural frequency of 833 Hz, a positive structural damping ratio (ζ_s) of 0.0015 (or 0.15%) would be required to prevent instability. Reference (5) states that this theory simply points out potential for instability rather than provide accurate estimates of onset of instability. To further examine flutter, a NASTRAN finite element analysis was conducted.

The NASTRAN flutter analysis was done for a flow velocity range of 0-2500 in/sec and $\beta=0$. Flow velocities of 0-250 inches/sec were of particular interest since they bound the test conditions. The results are shown in Figures 6 and 7. Table 2 summarizes the maximum negative damping due to the fluid flow for each mode which is an indication of the potential for instability. From Table 2, NASTRAN predicts that the first bending and first torsional modes are most likely to become unstable for the test conditions: A positive structural or viscous damper of at least 0.36% would be required to offset the negative damping. For Mode 5, at least 0.03% positive damping would be required. At higher flow velocities beyond the test conditions, four of the first six modes reach 0.5-0.85% negative damping due to the fluid.

5.0 DISCUSSION

The analysis results helped identify the mode that was excited during the test and how that mode was affected by additional hydromass. The analysis results have also provided an assessment of the potential for flutter instability of the plate extension. While negative damping was predicted due to flow over the plate extension, the amount of negative damping is considered low in comparison to typical positive

damping values. The modes analyzed were 1.0%-2.8% structurally damped in water. The predicted negative damping due to the fluid flow for Mode 5 does not exceed 0.03% at $V=250$ inches/sec (textbook solution predicted 0.15%). Furthermore, the predicted negative damping for that mode would not exceed 0.5% until the flow velocity exceeded 1000 inches/sec which is well beyond the range tested.

Based on the analytical results, the instability during the flow test was not due to a design feature of the plate extension. The analysis does not account for obstructions in the flow path which are present in a fully instrumented flow test. Therefore, contributions from these obstructions, such as instrumentation leads and/or devices, could have triggered the instability. This was confirmed with subsequent testing.

6.0 CONCLUSIONS

The fluid-structural instability experienced during flow testing in water has been analyzed using NASTRAN FEM. This analysis was conducted to predict which mode was being excited and to assess the stability of the structure. The results suggest that the design is fairly stable at flow velocities between 0-250 inches/sec. The fluid flow contributes only 0.00-0.36% negative damping which is less than typical positive structural damping in water. This suggested that the fluid-structural instability may not have been related to a design feature, but rather the test hardware. Further testing confirmed this suspicion and a costly redesign was spared since the instability was not related to a design feature.

7.0 ACKNOWLEDGMENTS

The author would like to acknowledge the following individuals for their important contributions to this work in this paper: Marty L. Pollack, Gene A. Terwilliger, and Rich S. Mendelson for their direct consultation; Rich A. Clarvit, Curt P. Gladding and Steve K. Cornelius for performing the experimental tests. The author would also like to thank Ron E. Otten and Ray Misiewicz for their support. Finally, the MacNeal Schwendler Corporation is thanked for allowing the use of NASTRAN aeroelasticity while this analysis was being conducted.

8.0 REFERENCES

- (1) F. Kreith, "Principles of Heat Transfer", Third Edition, Harper & Row Publishers, @ 1973
- (2) K.T. Patton, "Tables of Hydrodynamic Mass Factors for Translational motion," ASME Paper No. 65-WA/UNT-2
- (3) Ralph Brillhart, Pegasus XL Fin Dynamic Characterization for Flutter Evaluation, Proceedings of the 14th International Modal Analysis Conference, Society for Experimental Mechanics, @ 1996
- (4) D.R. Miller and R.G. Kennison, Theoretical Analysis of Flow-Induced Vibration of a Blade Suspended in a Flow Channel, ASME Paper No. 66 - WA / NE-1, @ 1966
- (5) R.D. Blevins, Flow Induced Vibration, First Edition, Van Nostrand Reinhold Company, @ 1977
- (6) MSC/NASTRAN Aeroelastic Analysis User Guide for Version 68, @ 1994, The MacNeal Schwendler Corp.

Table 1: NASTRAN Wet and Dry Normal Modes Analysis Results

Mode	Mode Shape	Dry Modal Frequency	Wet Modal Frequency	% Reduction
1	1st Bending in X	63.0	48.6	23%
2	1st Torsion about Z	324	276	15%
3	2nd Bending in X	394	318	19%
4	1st Bending in Y	502	496	1%
5	Complex Bending/Torsion*	992	833	16%
6	Complex Bending/Torsion	1100	941	14%

Table 2: Max. Negative Damping due to fluid flow ($\beta=0$)

Mode	Mode Shape	Flow Velocity for Max. Negative Damping (in/sec)	Max. Negative Damping Ratio (% Critical)	Max. Negative Damping Ratio between 0-250 in/sec (% Critical)
1	1st Bending in X	80	0.36	0.36
2	1st Torsion about Z	450	0.82	0.19
3	2nd Bending in X	550	0.60	0.13
4	1st Bending in Y	NS	NS	NS
5	Complex Bending/Torsion*	1300	0.60	0.03
6	Complex Bending/Torsion	1600	0.85	0.03

* - Mode believed to be associated with experimental instability
 NS - No significant negative damping predicted

FIGURE 5: Mode Shape for 833 Hz mode associated with fluid-structural instability in flow test

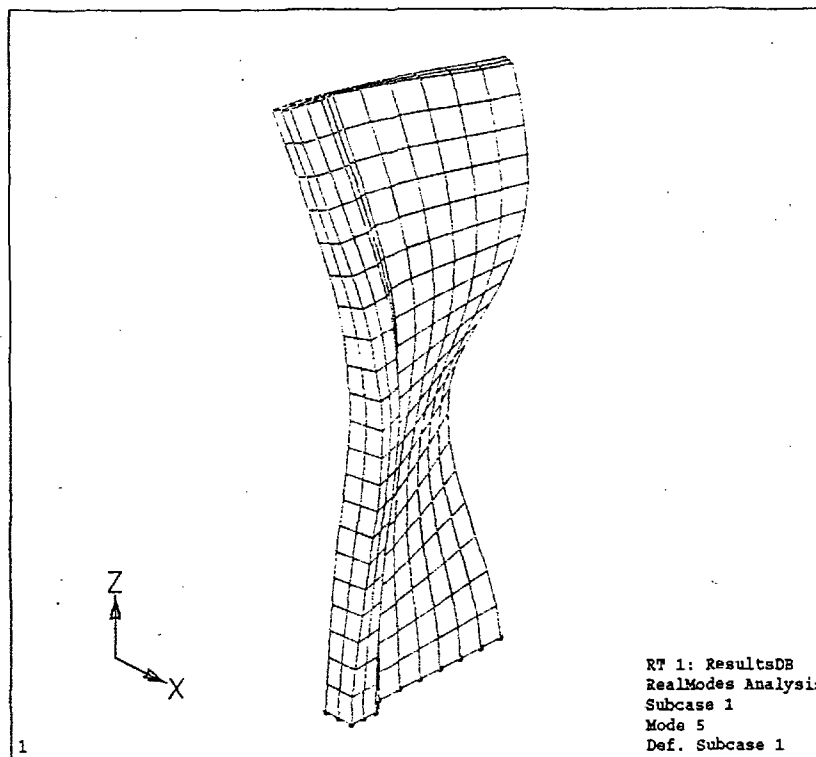


FIGURE 6: Damping and Frequency as a function of Flow Velocity for Modes 1-3

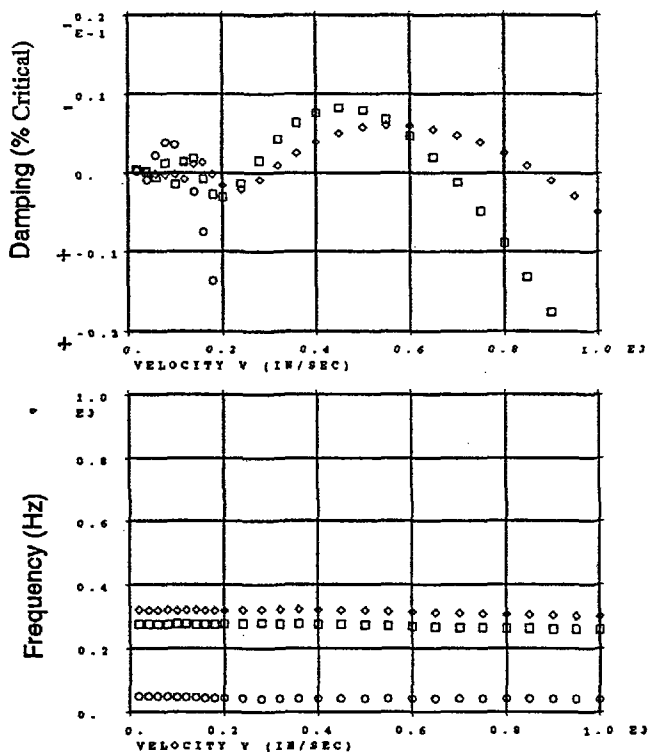
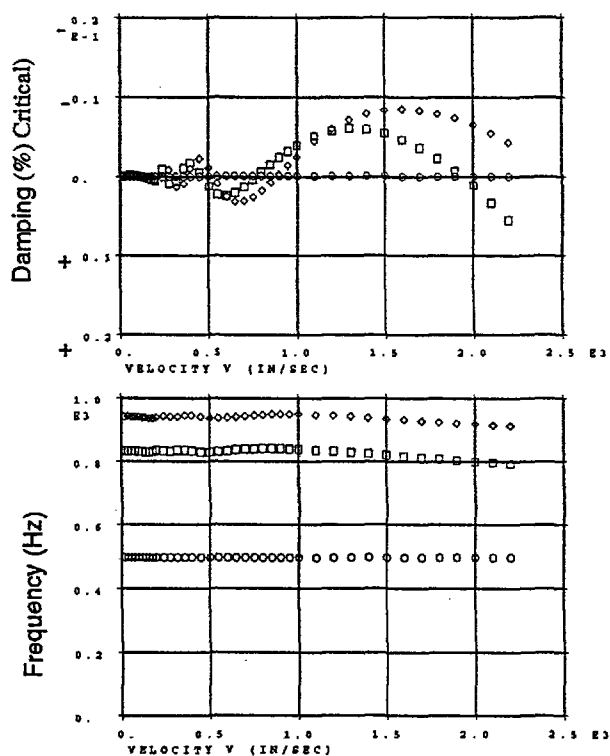


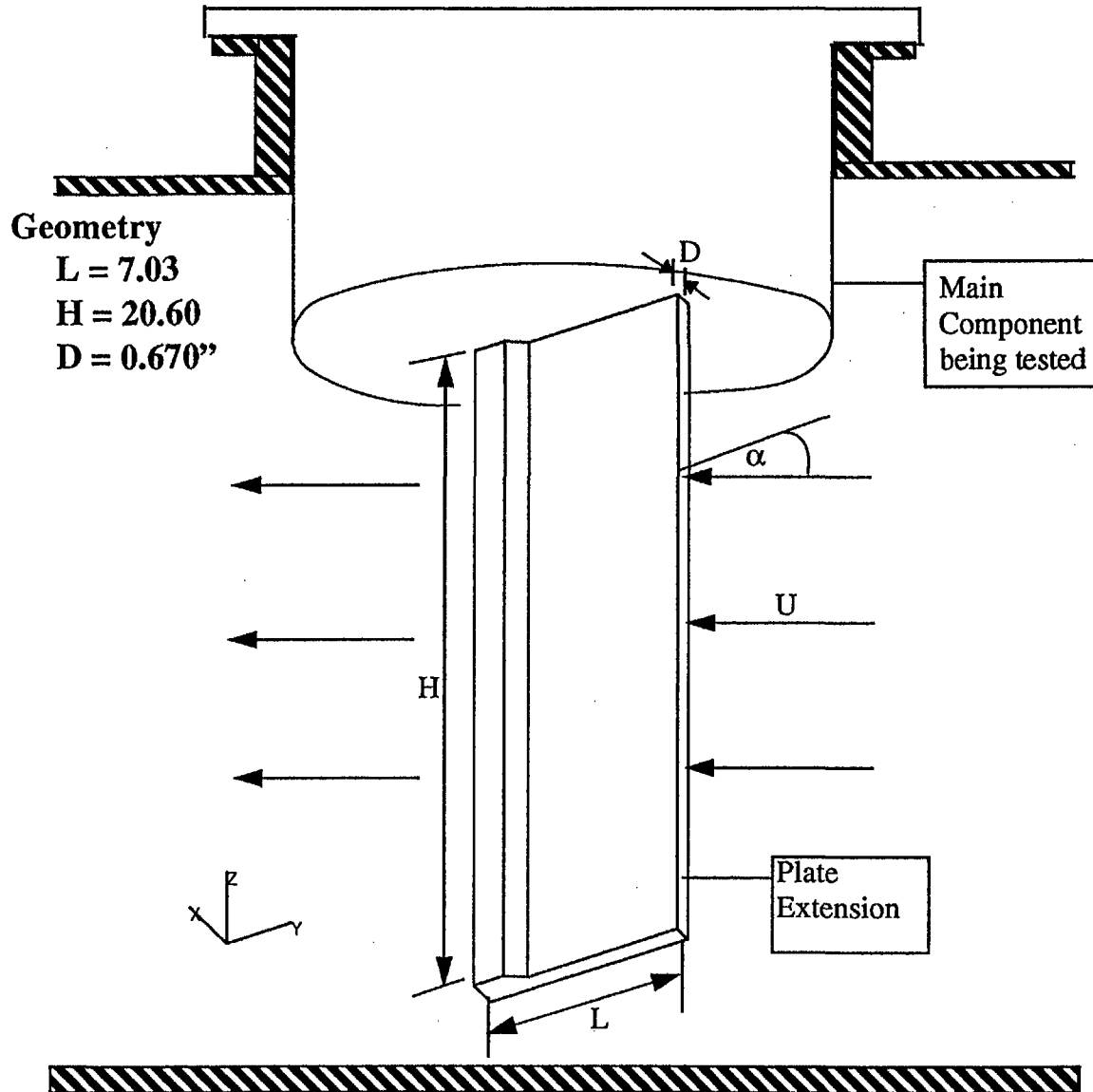
FIGURE 7: Damping and Frequency as a function of Flow Velocity for Modes 4-6





SUMMARY

1. INSTABILITY OBSERVED IN EXPERIMENTAL FLOW TEST IN WATER NEAR 800 Hz
 2. INSTABILITY ANALYSIS COMPLETED including:
 - Textbook Theory Evaluation
 - NASTRAN normal modes analyses
 - NASTRAN flutter analysis
-
3. MODAL ANALYSIS PREDICTED A 833 HZ COMPLEX BENDING/TORSIONAL MODE OF PLATE EXTENSION - ONLY MODE NEAR 800 HZ
 4. FLUTTER ANALYSES PREDICTED THAT THE COMPONENT DESIGN WAS NOT CONTRIBUTING TO THE INSTABILITY FOR THE GIVEN TEST CONDITIONS
 5. FURTHER TESTING ASSOCIATED INSTABILITY WITH TEST HARDWARE





EXPERIMENTAL CHARACTERISTICS OF FLUID-STRUCTURAL INSTABILITY

Experimental Characteristics:

- Sharp peaks occurred at a resonance frequency indicating low damping
- Slope of dB vs. Flow Rate curve developed high slopes
- Noise propagated to most accelerometers

Occurred for Structure Tested for the following conditions:

- ~ 800 Hz.
- Attack angle of -45° to $+45^{\circ}$
- High Temperature / High Pressure
- Cross Flow Rates = 90 - 180 inches / second



Figure 2: Spectra of Acceleration vs. Frequency at Different Flow Velocities

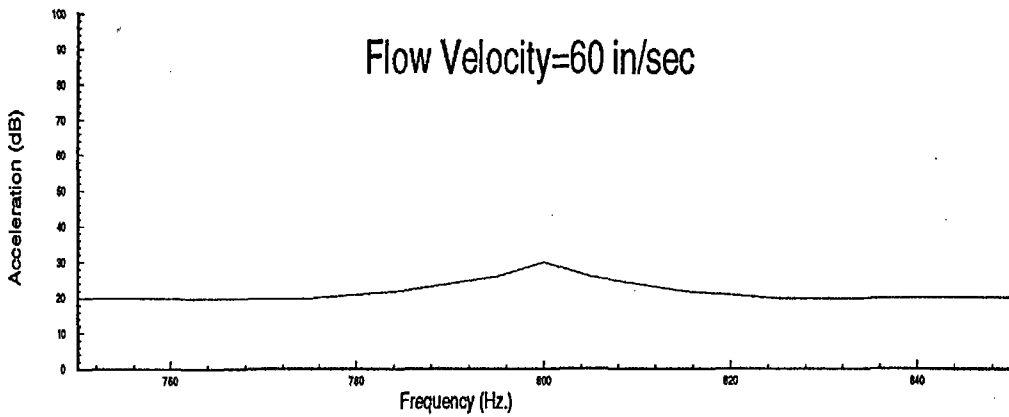
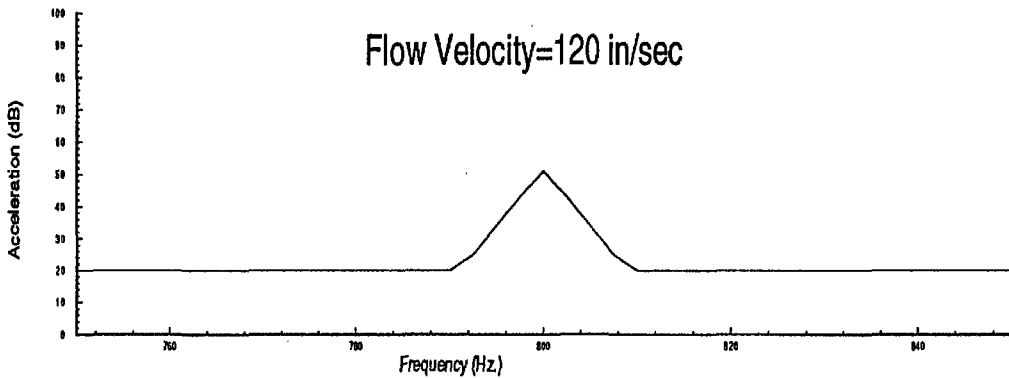
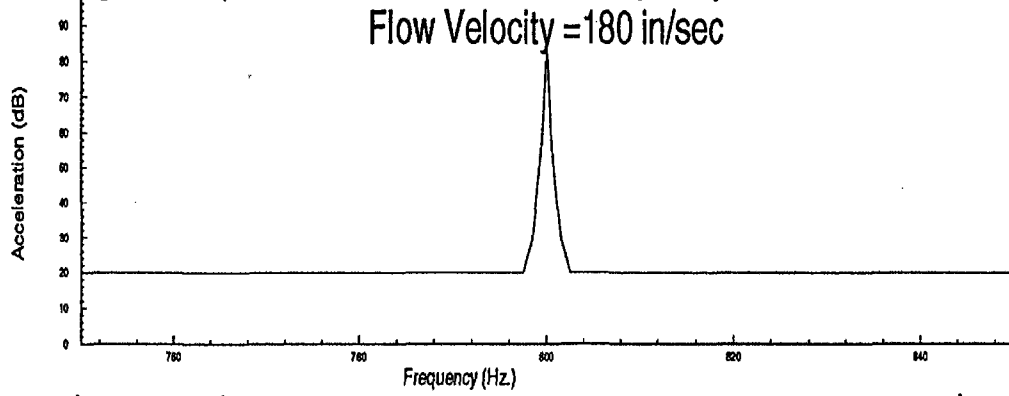
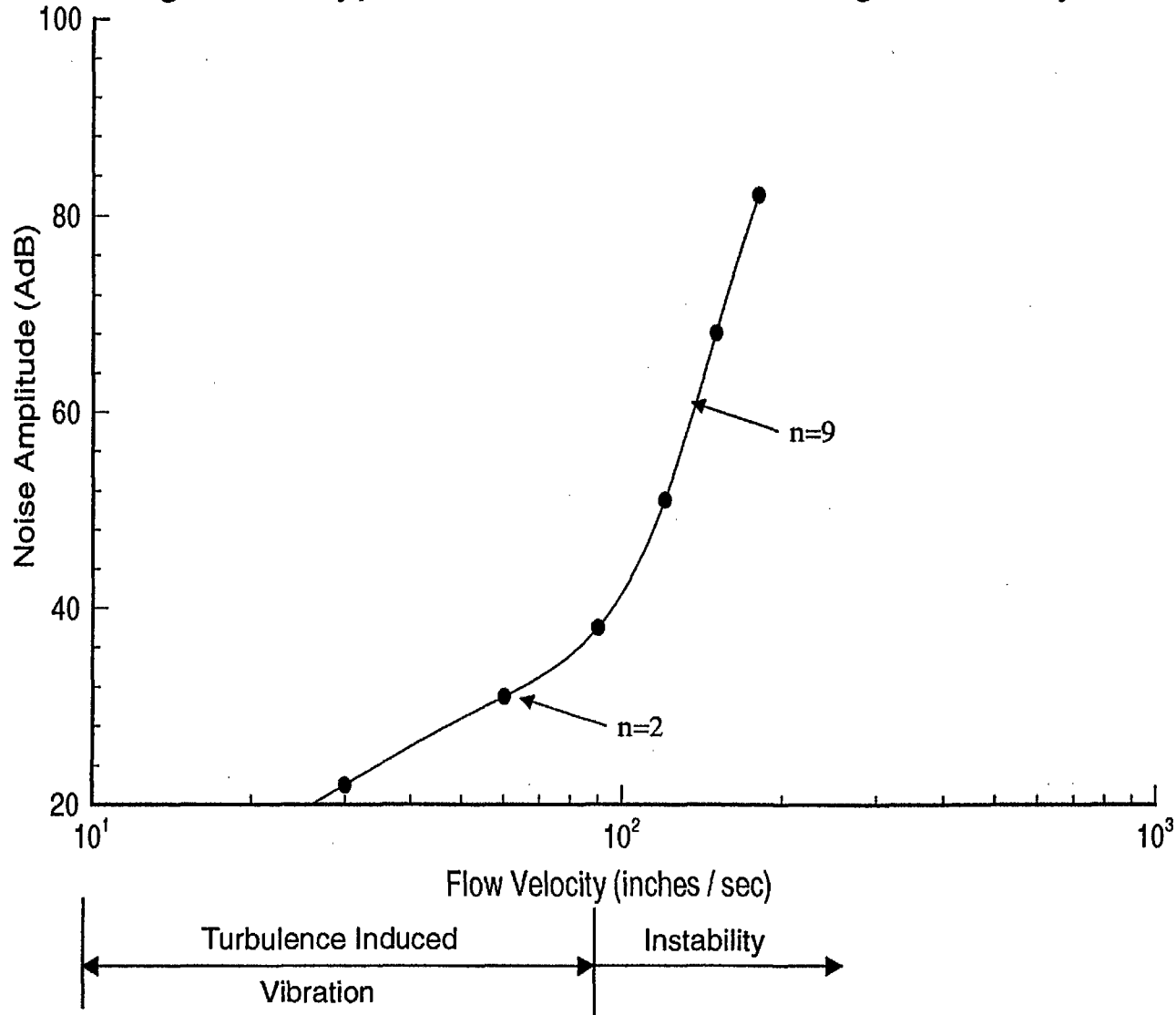




Figure 3: Typical Test Result Showing Instability





ANALYTICAL CHARACTERISTICS OF INSTABILITY

Instability occurs when the positive structural damping is offset by negative damping due to the fluid flow resulting in a net negative damping

The equation of motion is written for torsion and the fluid force as follows:

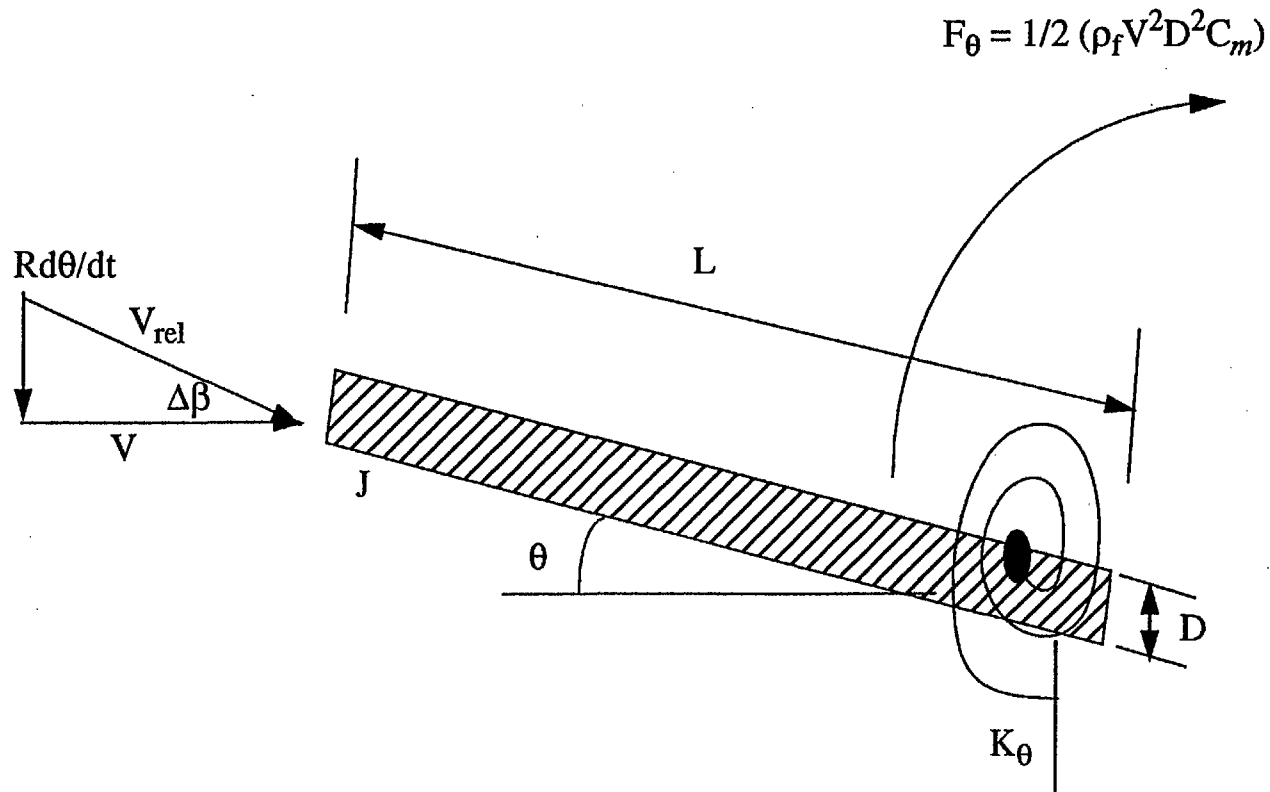
$$J \frac{d^2 \theta}{dt^2} + B \frac{d\theta}{dt} + K_\theta \theta = F(t) = \frac{\rho V^2 D^2 C_m}{2} = \frac{\rho V^2 D^2}{2} \left(C_M + \frac{\partial C_M}{\partial \beta} \beta \right)_{\beta=0}$$

$$J \frac{d^2 \theta}{dt^2} + \left(B - \frac{\rho V R D^2}{2} \left(\frac{\partial C_M}{\partial \beta} \right) \right) \frac{d\theta}{dt} + \left(K_\theta + \frac{\rho V^2 D^2}{2} \left(\frac{\partial C_M}{\partial \beta} \right) \right) \theta = 0$$

Instability occurs when $d\theta/dt$ terms reach zero resulting in the following relationship for the critical velocity:

$$\frac{V_c}{f_o \cdot D} = \left(\left(\frac{4\pi\rho_s \zeta_o}{3\rho_f} \right) \left(1 + \frac{L^2}{D^2} \right) \right) / \left(\frac{dC_M}{d\beta} \right)$$

Torsional Free Body Diagram for a Flat Plat subjected to a free stream flow



ANALYSIS RESULTS

NASTRAN Normal Modes Analysis:

- Predicted 833 Hz complex bending / torsion mode of plate extension in water

Textbook Theory Analysis:

- At $V=150$ inches /second, $\zeta_o = 0.0015$ or 0.15%

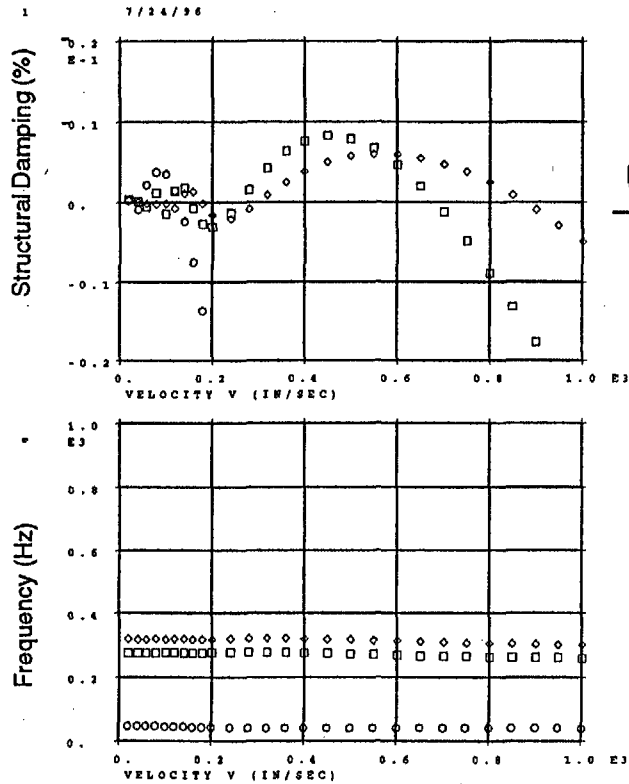
NASTRAN Flutter Analysis:

Mode	Mode Shape	Flow Velocity for Max. Negative Damping (in/sec)	Max. Negative Damping (% Critical)	Max. Negative Damping between 0-250 in/sec (% Critical)
1	1st Bending in X	80	0.36	0.36
2	1st Torsion about Z	450	0.82	0.19
3	2nd Bending in X	550	0.60	0.13
4	1st Bending in Y	NS	NS	NS
5	Complex Bending/Torsion*	1300	0.60	0.03
6	Complex Bending/Torsion	1600	0.85	0.03

* - Mode believed to be associated with experimental instability
 NS - No significant negative damping predicted

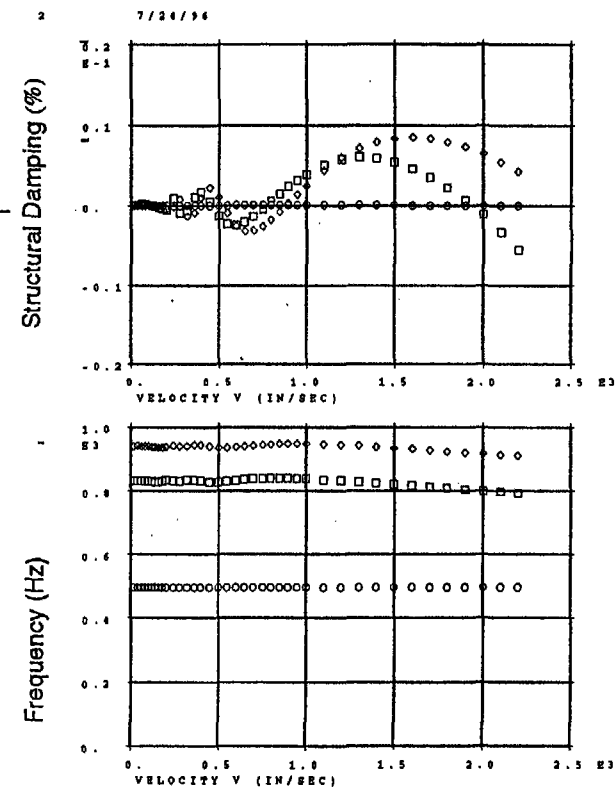


Damping and Frequency as a function of Flow Velocity for Modes 1-3



LATERAL REV. 6 FLUTTER ANALYSIS
 1/8 RIS
 PK-METHOD FLUTTER SOLUTION -- BASE RUN

Damping and Frequency as a function of Flow Velocity for Modes 4-6



LATERAL REV. 6 FLUTTER ANALYSIS
 1/8 RIS
 PK-METHOD FLUTTER SOLUTION -- BASE RUN

↑ Unstable
 ↓ Stable



DISCUSSION / CONCLUSIONS

- If modes analyzed are higher than 0.36% structurally damped, there would not be enough negative damping due to the fluid flow to cause an instability under the given test conditions
- Complex bending and torsional mode at ~800 Hz was only 0.03% negatively damped due to fluid flow up to 250 inches/sec
- Analysis predicted a fairly stable design at flow velocities between 0-250 inches/sec
- Test hardware (i.e. instrumentation) contributed to the instability
- A costly redesign was spared since the instability was not related to a design feature